TMR

ARTICLE

Traditional Medicine Research 2026;11(3):17. http://doi.org/10.53388/TMR20241224001

Ameliorative effect of ononin on the inflammatory response in doxorubicin-induced acute kidney injury mice

Qing-Xi Hu[1#], Xin-Ting Zhang[1#], Shi-Qi Zhang[1], Ya-Shu Li[1], Hai-Qiang Zhang[2*], Jiao Liu[1*], Jie Cheng[1, 2*]

[1]Graduate School, Hebei University of Chinese Medicine, Shijiazhuang 050000, China. [2]Laboratory of Evaluation and Transformation of Traditional Chinese Medicine Under Hebei Provincial Administration of Traditional Chinese Medicine, Hebei Provincial Hospital of Chinese Medicine, Shijiazhuang 050000, China.

[#]These authors contributed equally to this work and are co-first authors for this paper.

[*]**Correspondence to:** Hai-Qiang Zhang, Laboratory of Evaluation and Transformation of Traditional Chinese Medicine Under Hebei Provincial Administration of Traditional Chinese Medicine, Hebei Provincial Hospital of Chinese Medicine, No. 389, Zhongshan East Road, Chang'an District, Shijiazhuang 050000, China. E-mail: zhanghaiqiangdyx@163.com. Jiao Liu, Jie Cheng, Graduate School, Hebei University of Chinese Medicine, No. 326, Xinshi South Road, Qiaoxi District, Shijiazhuang 050000, China. Email: fairypc_lj@163.com; jiechengyx2024@163.com.

Author contributions

Hu QX and Zhang XT performed the experiments and wrote the manuscript. Zhang SQ and Li YS performed the data analyses. Zhang HQ, Liu J and Cheng J provided supervision and contributed to writing, review, and editing.

Competing interests

The authors declare no conflicts of interest.

Acknowledgments

The work was supported by Hebei Province Natural Science Foundation (H2023423037); The Government Funded Clinical Program of Hebei Province (No. ZF2025287); Special Project of Hebei Industrial Technology Institute for Traditional Chinese Medicine Preparation (No. YJY2024001); Chinese Medicine Scientific Research Program of Hebei Province (No. 2025222).

Peer review information

Traditional Medicine Research thanks Jiao-Jiao Fan and other anonymous reviewers for their contribution to the peer review of this paper.

Abbreviations

AKI, acute kidney injury; RRT, renal replacement therapy; HRP, Horseradish peroxidase; PPI, protein-protein interaction; GO, gene ontology; RSI, renal somatic index; TEM, transmission electron microscopy; DXMS, Dexamethasone; HE, hematoxylin and eosin; PAS, periodic acid-Schiff; MASSON, Masson's trichrome; IF, immunofluorescence; WB, western blot.

Citation

Hu QX, Zhang XT, Zhang SQ, et al. Ameliorative effect of ononin on the inflammatory response in doxorubicin-induced acute kidney injury mice. *Tradit Med Res.* 2026;11(3):17. doi: 10.53388/TMR20241224001.

Executive editor: Meng-Meng Song.

Received: 25 December 2024; **Revised:** 25 March 2025; **Accepted:** 03 June 2025; **Available online:** 01 July 2025.

Abstract

Background: Acute kidney injury (AKI), characterized by rapid renal dysfunction (KDIGO 2022 criteria: 48-hour doubling of serum creatinine or < 0.5 mL/kg/h urine output for > 6 h), affects 13.3 million people annually with > 20% mortality. Its progression involves metabolic imbalances, toxin accumulation, and multiorgan failure, often culminating in chronic kidney disease. Current therapies (fluid resuscitation, diuretics, renal replacement therapy) remain limited. Inflammation drives AKI pathogenesis: renal insults (ischemia, toxins) trigger tubular cell release of pro-inflammatory mediators (TNF-α, IL-1β, IL-6), activating neutrophil gelatinase-associated lipocalin (NGAL) and dysregulating P38 MAPK/ERK pathways. This cascade promotes leukocyte infiltration, oxidative stress, and apoptosis, exacerbating renal damage. Ononin, a flavonoid from *Astragali Radix*, shows multi-target potential by suppressing pro-inflammatory cytokines, modulating signaling, and mitigating oxidative stress. Its dual anti-inflammatory/antioxidant properties position it as a promising candidate for AKI intervention. Exploring the ameliorative effect of ononin on the inflammatory response Ameliorative effect of ononin on the inflammatory response in doxorubicin-induced AKI mice. **Methods:** We used network pharmacology to explore ononin's target molecules and AKI-related disease molecules, identified their intersections, and predicted potential mechanisms via enrichment analysis, followed by molecular docking verification. For in-vivo validation, 50 mice were randomly divided into five groups (n = 10/group): Control, Model, Ononin-L (15 mg/kg), Ononin-H (60 mg/kg), and Dexamethasone (2.6 mg/kg). An AKI model was established by intravenous tail-vein injection of Doxorubicin (15 mg/kg). Samples were collected 12 h post-induction. We calculated the renal coefficient, examined renal histopathology using hematoxylin and eosin (HE), periodic acid-Schiff (PAS), and Masson's trichrome (MASSON) staining, and observed mitochondrial morphology by electron microscopy (EM). ELISA was used to measure NGAL, serum creatinine (Scr), and blood urea nitrogen (BUN) levels in serum. Immunofluorescence (IF) evaluated the expression of P-P38, P-ERK, NGAL, and KIM-1 in renal tissues. RT-qPCR assessed the gene expression of pro-inflammatory cytokines, MAPK pathway components, and renal injury markers in kidney tissues. Western Blot (WB) quantified P-P38, P38 MAPK, P-ERK, ERK, NGAL, and KIM-1 in renal tissues. **Results:** Network pharmacology analysis suggested that ononin could attenuate AKI through its anti-inflammatory properties and regulation of the MAPK signaling pathway. The Model group exhibited a significantly elevated renal coefficient ($P < 0.05$), severe histopathological damage, and mitochondrial dysfunction compared to controls. Serum levels of NGAL, Scr, and BUN were markedly increased ($P < 0.05$), indicating impaired renal function. Enhanced fluorescence signals of P-P38 MAPK, P-ERK, NGAL, and KIM-1 suggested activation of MAPK pathways and renal injury. Upregulation of pro-inflammatory cytokines (*IL-1β*, *IL-6*, *TNF-α*) and MAPK-related genes (*P38 MAPK*, *ERK*) alongside injury markers (*NGAL*, *KIM-1*) ($P < 0.05$). Increased ratios of phosphorylated-to-total proteins (P-P38/P38, P-ERK/ERK) and elevated NGAL/KIM-1 protein levels confirmed pathway dysregulation. Treatment significantly reduced the renal coefficient ($P < 0.05$), attenuated histological damage, and restored mitochondrial integrity. NGAL, Scr, and BUN levels were lowered, reflecting functional recovery. Diminished fluorescence intensities of P-P38, P-ERK, NGAL, and KIM-1 indicated suppression of injury pathways. Downregulation of inflammatory cytokines (*IL-1β*, *IL-6*, *TNF-α*), MAPK components (*P38 MAPK*, *ERK*), and injury markers (*NGAL*, *KIM-1*) ($P < 0.05$). Reduced phosphorylation ratios (P-P38/P38, P-ERK/ERK) and decreased NGAL/KIM-1 protein expression demonstrated therapeutic efficacy. **Conclusion:** Ononin ameliorates inflammatory responses in AKI mice via the P38 MAPK/ERK pathway.

Keywords: ononin; acute kidney injury; inflammation; doxorubicin

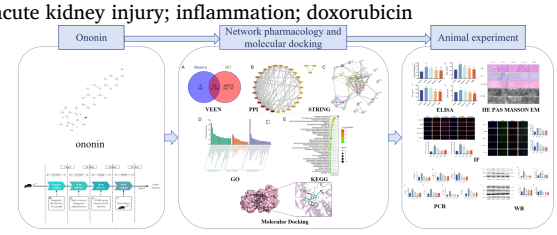

Traditional Medicine Research 2026;11(3):17. http://doi.org/10.53388/TMR20241224001

Highlights

1. Ononin treats AKI through its anti-inflammatory mechanisms.
2. Integrated network pharmacology prediction, molecular docking, and murine model validation with multi-omics assessments were used.
3. Ononin is associated with the MAPK pathway.
4. Ononin achieves the goal of treating AKI by inhibiting P38 MAPK/ERK phosphorylation and reducing inflammatory response.

Medical history of objective

Ononin, a flavonoid from *Astragali Radix* (Huangqi), has been historically documented in traditional Chinese medicine (TCM) for its dual anti-inflammatory and antioxidant properties. First described in *the Shennong Bencao Jing* (ca. 200–250 C.E.), *Astragali Radix* was classified as a "superior herb" for its ability to "tonify Qi (In traditional Chinese medicine, "Qi" refers to the fundamental energy that constitutes the human body and sustains life activities, while also embodying the concept of physiological functions.), resolve edema, and promote tissue repair" – functions now linked to ononin's molecular mechanisms. In the Ming Dynasty, Li Shizhen's *Bencao Gangmu* (1596 C.E.) further emphasized its use in "clearing heat-toxin and alleviating urinary disorders," aligning with modern observations of ononin's nephroprotective effects. Recent pharmacological studies reveal that ononin suppresses pro-inflammatory cytokines, modulates signaling pathways (e.g., MAPK/ERK), and mitigates oxidative stress, positioning it as a promising candidate for AKI intervention.

Introduction

Acute kidney injury (AKI) represents a sudden deterioration of renal function, typically developing over hours to days and persisting for at least 24 h. In 2022, the Kidney Disease: Improving Global Outcomes (KDIGO) working group defined AKI as either a doubling of Scr within 48 h or a persistent reduction in urine output to less than 0.5 mL/kg/h for more than 6 h [1]. The occurrence of AKI is often accompanied by disturbances in water-electrolyte balance, acid-base imbalances, impaired excretion of toxic substances, and ultimately multiorgan failure, which can directly result in End-Stage Renal Disease (ESRD) and increase the risk of developing or exacerbating Chronic Kidney Disease [2]. Annually, over 13.3 million people worldwide are affected by AKI, with a mortality rate exceeding 20% [3]. Effective pharmaceutical strategies for AKI prevention and treatment remain an unresolved challenge in nephrology. For early-stage patients, interventions such as intravenous fluid administration, colloid therapy, or diuretic treatment may be employed; however, these approaches are associated with significant adverse effects and are unsuitable for end-stage patients. For patients with ESRD or severe AKI, renal replacement therapy (RRT) is often necessary, although the optimal timing of RRT initiation remains under investigation [4]. Developing effective AKI therapeutics remains an urgent biomedical priority requiring multidisciplinary solutions. Despite significant advancements in understanding AKI pathogenesis, effective pharmacological treatments remain elusive. Emerging research has demonstrated the therapeutic promise of bioactive phytochemicals originating from traditional Chinese medicine, which exhibit protective effects against acute kidney injury via dual modulation of inflammatory cascades and oxidative stress pathways.

Inflammation is a fundamental pathological process wherein biological tissues respond to various injury factors, including trauma and infection [5]. Inflammatory responses constitute a central role in the initiation and progression of AKI, representing one of the pathogenic mechanisms [6]. When the kidney is subjected to a variety of injury factors, including ischemia-reperfusion injury, toxic substances exposure, immune-mediated damage or other pathological conditions, the inflammatory response is activated, thereby exacerbating renal tissue damage. During the initial phase of AKI, injured renal cells release multiple inflammatory mediators, including TNF-α, IL-1β and IL-6, which recruit and activate NGAL (a well-established biomarker of AKI), thereby amplifying the inflammatory response [7–9]. Accumulating evidence has demonstrated that NGAL expression is closely linked to the P38 MAPK/ERK signaling pathway [10, 11]. Dysregulated P38 MAPK/ERK signaling has been established as a pivotal driver of inflammatory cascades and functional decline in AKI, promoting tubular epithelial cell apoptosis and leukocyte infiltration. Specifically, P38 MAPK/ERK activation induces infiltration of neutrophils and macrophages, resulting in renal tissue inflammation, oxidative stress, and cellular apoptosis, which collectively contribute to renal dysfunction exacerbation [12, 13]. Mitochondrial dysfunction leads to renal tubular epithelial cell damage, thereby contributing to renal function impairment and AKI development [14]. These findings collectively indicate that inflammatory responses significantly contribute to AKI progression, and that targeted modulation of inflammation represents a promising therapeutic strategy for AKI management. Furthermore, anti-inflammatory therapies show substantial potential for clinical development in AKI treatment.

Ononin, a biologically active flavonoid compound derived from traditional Chinese medicine herbs including *Astragali Radix*, exhibits multiple pharmacological activities such as free radicals scavenging, anti-oxidant, anti-tumor, anti-inflammatory effects as well as protection against ischemia-reperfusion injury [15]. Experimental studies have demonstrated that ononin effectively ameliorates cognitive dysfunction via its anti-inflammatory and antioxidant properties in Alzheimer's disease mouse models [16]. Furthermore, ononin significantly downregulates the expression of TNF-α, IL-1β, and IL-6, thereby attenuating inflammatory responses. Additionally, it demonstrates anti-apoptotic effects [17]. Recent investigations have confirmed that ononin effectively inhibits pro-inflammatory cytokine production and modulates the MAPK signaling pathway [18]. Collectively, these findings indicate that ononin exerts therapeutic effects on inflammatory diseases. Given that AKI pathogenesis is largely mediated by inflammatory processes, ononin represents a promising therapeutic agent for AKI-associated inflammation.

Therefore, the study seeks to elucidate the nephroprotective effects of ononin against AKI by systematically evaluating its capacity to: Attenuate pro-inflammatory cytokine storms (IL-1β/IL-6/TNF-α), Restore P38 MAPK/ERK signaling homeostasis, Mitigate histopathological renal damage in established murine AKI models.

Materials and methods

Materials

Veterinary drug. Ononin (purity > 98%, lot number DST231204-044) was purchased from Chengdu Desite Biotechnology Co., Ltd. (Chengdu, China). Dexamethasone (lot number D2305301) was purchased from Xinxiang Changle Pharmaceutical Co., Ltd. (Xinxiang, China). Doxorubicin (lot number B23031137) was purchased from Aladdin Scientific Corporation (Shanghai, China).

Main chemical reagents. Commercial assay kits and antibodies were sourced as follows: NGAL ELISA Kit (BBI Life Sciences Corporation (Hong Kong, China), Lot D721123), Scr/BUN Detection Kits (Beckman Coulter, Inc. (Brea, CA, USA), Lots AUZ3562/AUZ3611), Horseradish peroxidase (HRP)-conjugated secondary antibodies (Abbkine Biotechnology Co., Ltd. (Wuhan, China), Cat A21010/A21020), MAPK pathway antibodies (P38/ERK total/phospho-forms, Proteintech Group, Inc. (Wuhan, China)), Renal injury markers (KIM-1: Proteintech Group, Inc. (Wuhan, China), 83221-2-RR; NGAL: Immunoway Biotechnology Company (Nanjing, China) YT7910).

Instruments. The electronic balance was purchased from METTLER TOLEDO International Inc. (Greifensee, Switzerland). The TGL-16R refrigerated centrifuge was purchased from Shandong BaiO Medical Technology Co., Ltd. (Jinan, China). The TGL-16R refrigerated grinder was purchased from Shanghai Jingxin Industrial Development Co., Ltd. (Shanghai, China). The Vortex-Genie 2 vortex oscillator was

purchased from Scientific Industries, Inc. (Bohemia, NY, USA). The SMB-H thermostatic Metal Dry Bath was purchased from Servicebio Biotechnology Co., Ltd. (Wuhan, China). The 7500 real-time PCR instrument was purchased from Thermo Fisher Scientific Inc. (Waltham, MA, USA). The EP600 electrophoresis power supply, PRO4 mini vertical gel tank, and mini protein transfer system were purchased from WIX Technology (Beijing) Co., Ltd. (Beijing, China). The Ultra-micro ultraviolet-visible spectrophotometer was purchased from Hangzhou Miu Instruments Co., Ltd. (Hangzhou, China).

Network pharmacology and molecular docking

Target screening of ononin. The molecular structure of ononin was retrieved from PubChem (http://pubchem.ncbi.nlm.nih.gov/). Its potential therapeutic targets were predicted using SwissTargetPrediction (http://www.swisstargetprediction.ch; organism: Homo sapiens) and GeneCards databases (http://www.genecards.org), followed by data integration and redundancy removal.

Acquisition of AKI-related targets. The keywords "acute kidney injury" were used to search for potential targets in the OMIM (http://www.omim.org/), DisGeNET (http://disgenet.com/) and GeneCards (http://www.genecards.org; organism: Homo sapiens) databases.

Screening for potential targets of ononin in the treatment of AKI and construction of a protein interaction network. Potential therapeutic targets of ononin were cross-referenced with known AKI-associated targets using the Venny 2.1 platform (https://bioinfogp.cnb.csic.es/tools/venny/index.Html), generating an intersection set visualized via Venn diagram.

The target list was analyzed using STRING (http://cn.string-db.org/) to construct a protein-protein interaction (PPI) network, which was then visualized and topologically analyzed in Cytoscape with the degree centrality algorithm identifying hub targets.

Enrichment analysis of core targets. Functional enrichment analysis of overlapping targets was conducted via Metascape (http://metascape.org/gp/index.html#/main/step1), with Gene Ontology (GO) biological processes and KEGG pathways analyzed using default parameters. The results were visualized as bar charts and bubble charts using the Micro Life Letter platform (http://www.bioinformatics.com.cn/).

Enrichment analysis of core targets. The genes of core targets for the effective ingredients in treating diabetic wounds were imported into the DAVID database (http://david.ncifcrf.gov). The species was set to "Homo sapiens," and GO annotation and KEGG pathway enrichment analyses were performed. The data were visualized using a bioinformatics platform.

Molecular docking of core targets. The 3D structure of ononin was obtained from the PubChem database (http://pubchem.ncbi.nlm.nih.gov/) using the compound name as the search keyword.

Key proteins were searched in the PDB database (http://www.rcsb.org/) and filtered for those with a resolution below 2 A and containing ligands. Molecular docking predictions between the screened proteins and ononin were performed using the HDOCK server (http://hdock.phys.hust.edu.cn/). The results were visualized using PyMOL software to analyze receptor-ligand interactions.

Animal experiment

Animals. Male C57BL/6 mice (18–22 g, 8 week, specific pathogen-free) were procured from the accredited Laboratory Animal Center of Hebei University of Chinese Medicine (SYXK 2023-012) and maintained under SPF conditions. Animals were housed under constant environmental conditions (22 ± 2 ˚C) and were given ad libitum access to water and food. All animal procedures strictly adhered to China's national guidelines for experimental animal welfare and were approved by the Institutional Animal Care and Use Committee (HBZY2023-YS-232-01).

Dose and group design. Fifty C57BL/6 mice were randomly allocated into five experimental arms (n = 10/group): Untreated Control, Disease Model (AKI-induced), Ononin treatment (15 mg/kg, low-dose), Ononin treatment (60 mg/kg, high-dose), Positive Control (Dexamethasone, DXMS, 2.6 mg/kg). The compound was solubilized in sterile physiological saline (0.9% w/v NaCl) to achieve the desired concentration for administration. Ononin groups received daily oral ononin (15 or 60 mg/kg) for 14 consecutive days, while model controls were given vehicle (0.9% NaCl). On day 14, dexamethasone (2.6 mg/kg) was administered intraperitoneally. Adriamycin-induced AKI (15 mg/kg, i.v.) was initiated 1h post-final treatment in all groups except naïve controls. After 12 h of fasting without water, sampling was performed on the following day. The experimental time flow diagram is displayed in Figure 1.

Sampling and kidney index. On day 15 of the experiment, animals were anesthetized by intraperitoneal administration of 2% sodium pentobarbital. Blood specimens were obtained via retro-orbital venous plexus puncture and permitted to coagulate at room temperature for 30 min. Subsequent centrifugation at 3,000 rpm for 15 min (4 ˚C) yielded serum, which was aliquoted and preserved at −80 ˚C until analysis. After blood collection, quickly sever the cervical spine and execute the patient. The abdominal cavity was surgically opened along the midline, and both kidneys were promptly excised. After gently removing residual blood from the surface with sterile filter paper, the kidneys were weighed using an analytical balance, and the weights were recorded. Renal tissues were systematically processed for diverse analytical approaches: immersion in 4% paraformaldehyde (PFA) at ambient temperature for histopathological examination, preservation in 2.5% glutaraldehyde solution for ultrastructural analysis via electron microscopy, and immediate cryopreservation in liquid nitrogen followed by storage at −80 ˚C for molecular studies. The renal somatic index (RSI) was computed as the percentage ratio of combined kidney mass (milligrams) to total body weight (grams). [(Bilateral Kidney Weight / Body Weight) × 100%)].

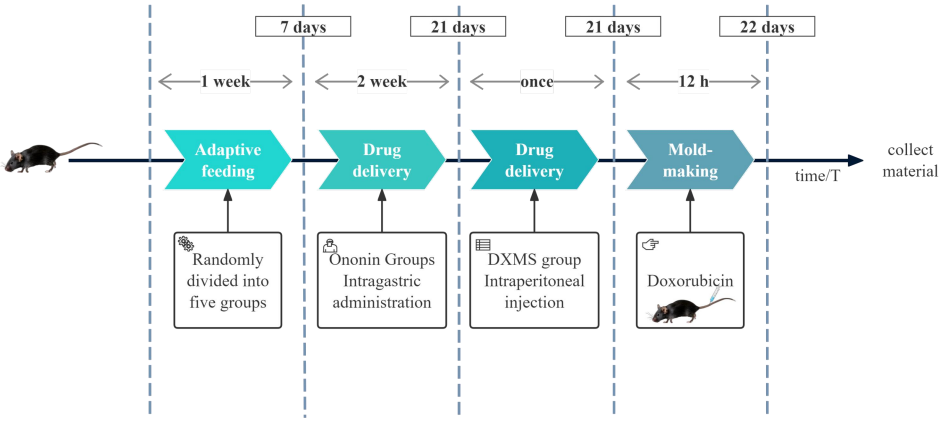

Figure 1 Experiment time flow chart. DXMS, Dexamethasone.

Serum biochemical parameter measurement. Concentrations of NGAL, Scr, and BUN in serum samples were determined through enzyme-linked immunosorbent assay (ELISA) and conventional biochemical techniques, in strict accordance with the manufacturer's recommended procedures.

Hematoxylin eosin, periodic acid-Schiff and MASSON staining. Renal specimens were immersed in 4% paraformaldehyde (PFA) and fixed for 48 h at 4 ˚C. Following fixation, tissues underwent sequential dehydration in an ascending ethanol gradient (70%–100%), followed by xylene clearing and paraffin impregnation. Embedded tissues were sectioned at 4 μm thickness with a rotary microtome (Leica RM2235). Sections were subjected to hematoxylin and eosin (HE), periodic acid-Schiff (PAS), and Masson's trichrome staining according to conventional histochemical protocols. Microscopic evaluation was performed using a Nikon Eclipse E100 brightfield microscope equipped with a digital camera system for image acquisition and pathological assessment.

Electron microscopy. The mouse kidney was embedded using an electron microscopy fixative, and ultrathin sections of 80 nm were prepared. Ultrathin sections were subjected to dual heavy metal staining, first with uranyl acetate followed by lead citrate treatment, to enhance contrast for ultrastructural analysis. Mitochondrial architecture was then examined using transmission electron microscopy at appropriate magnifications.

Immunofluorescence. Kidney tissues from different experimental groups were processed into 4-μm thick paraffin sections. Paraffin-embedded tissue sections underwent sequential processing beginning with xylene-mediated deparaffination, followed by gradual rehydration through descending ethanol concentrations (100% to 70%). Antigen epitopes were unmasked through microwave-assisted heat-induced epitope retrieval (HIER) using sodium citrate buffer (PH 6.0). Non-specific binding sites were blocked with 5% bovine serum albumin (BSA) prior to overnight incubation with primary antibodies at 4 ˚C. Secondary antibody conjugation was performed for 60 min at room temperature. Between each immunostaining step, sections were thoroughly washed with PBS-T (0.1% Tween-20 in phosphate-buffered saline, pH 7.4) in four 5-min cycles. Following nuclear counterstaining, tissue sections were coverslipped using a fluorescence-preserving mounting medium supplemented with a photobleaching inhibitor, with all procedures conducted under light-protected conditions to prevent fluorophore degradation. Fluorescence microscopy was then used to observe and capture images of the tissue sections to examine the fluorescent expression of P-P38 MAPK, P-ERK, NGAL and KIM-1 proteins.

Real-time quantitative PCR. Total RNA was isolated from renal tissues utilizing a commercial RNA extraction kit. Subsequent cDNA synthesis was performed via reverse transcription. Gene-specific primer pairs were custom-designed and commercially synthesized for quantitative real-time PCR amplification targeting inflammatory cytokines (*IL-1β*, *IL-6*, *TNF-α*), MAPK pathway components (*P38 MAPK*, *ERK*), and renal injury markers (*NGAL*, *KIM-1*). Relative mRNA expression levels were calculated using the comparative $2^{-\Delta\Delta Ct}$ method, with primer sequences detailed in Table 1.

Western blot (WB). Tissue specimens were homogenized in RIPA lysis buffer containing protease inhibitor cocktail. Total protein content was determined via bicinchoninic acid (BCA) assay. Equal protein aliquots (20–50 μg) were resolved by 10% SDS-polyacrylamide gel electrophoresis under reducing conditions, followed by electrophoretic transfer to PVDF membranes pre-treated with methanol. Membranes were blocked with 5% non-fat milk/TBST for 1 h at room temperature, then probed with primary antibodies (diluted in blocking buffer) at 4 ˚C overnight. Following four 6-min TBST washes, membranes were incubated with HRP-conjugated secondary antibodies (1:5,000) for 50 min at room temperature. After repeated washing, protein bands were visualized using enhanced chemiluminescence (ECL) substrate and quantified with ImageJ software (NIH).

Statistical analysis

Statistical analyses were performed using GraphPad Prism version 8.0.2 (GraphPad Software, San Diego, CA, USA). Continuous variables with normal distribution were expressed as mean ± standard deviation (SD) and analyzed by one-way ANOVA with post-hoc testing. For non-normally distributed data, results were presented as median with interquartile range (IQR) and evaluated using non-parametric tests (Mann-Whitney U test for two-group comparisons or Kruskal-Wallis H test for multiple groups). All experiments included a minimum of three biological replicates. A two-tailed *P*-value < 0.05 was considered statistically significant.

Results

Network pharmacology analysis

Through comprehensive bioinformatics analysis employing both SwissTargetPrediction and GeneCards platforms, we successfully predicted 36 putative molecular targets associated with ononin. Furthermore, 10,405 targets associated with AKI were retrieved from OMIM, DisGeNET, and GeneCards databases.

Bioinformatic analysis employing Venny 2.1 revealed 33 common targets at the intersection of ononin's predicted molecular targets and known AKI-associated genes, suggesting these shared targets may mediate ononin's nephroprotective effects (Figure 2A).

The PPI network was constructed using STRING database, resulting in a network with 30 nodes and 105 edges (Figure 2B). The PPI network was then analyzed for topological properties using Cytoscape, ranking the target proteins in the PPI network based on their degree centrality values (Figure 2C). Based on network topology parameters (degree, closeness, and betweenness centrality), 13 core targets were identified: ABL1, IL2, MAPK14 (P38 MAPK), STAT3, TP53, KIT, VCAM1, TNF, SRC, BRCA1, CA9, PECAM1, and SELE.

Table 1 Primer sequences for target genes in PCR

Oligo name	Sequence (5' to 3')
GAPDH-M-F	ACTCCACTCACGGCAAATTCAAC
GAPDH-M-R	ACACCAGTAGACTCCACGACATAC
IL1β-M-F	TCGCAGCAGCACATCAACAAGAG
IL1β-M-R	AGGTCCACGGGAAAGACACAGG
IL-6-M-F	CTTCTTGGGACTGATGCTGGTGAC
IL-6-M-R	AGGTCTGTTGGGAGTGGTATCCTC
TNF-M-F	GCCTCTTCTCATTCCTGCTTGTGG
TNF-M-R	GTGGTTTGTGAGTGTGAGGGTCTG
P38 MAPK-M-F	TGTGATTGGTCTGTTGGATGTGTTC
P38 MAPK-M-R	TGGCACTTCACGATGTTGTTCAG
ERK-M-F	TGTTCCCAAATGCTGACTCCAAAG
ERK-M-R	AGCCTGTTCAACTTCAATCCTCTTG
NGAL-M-F	AGGGCTGTCGCTACTGGATCAG
NGAL-M-R	CGAACTGGTTGTAGTCCGTGGTG
KIM-1-M-F	CCTGCTGCTACTGCTCCTTGTG
KIM-1-M-R	CGGAAGGCAACCACGCTTAGAG

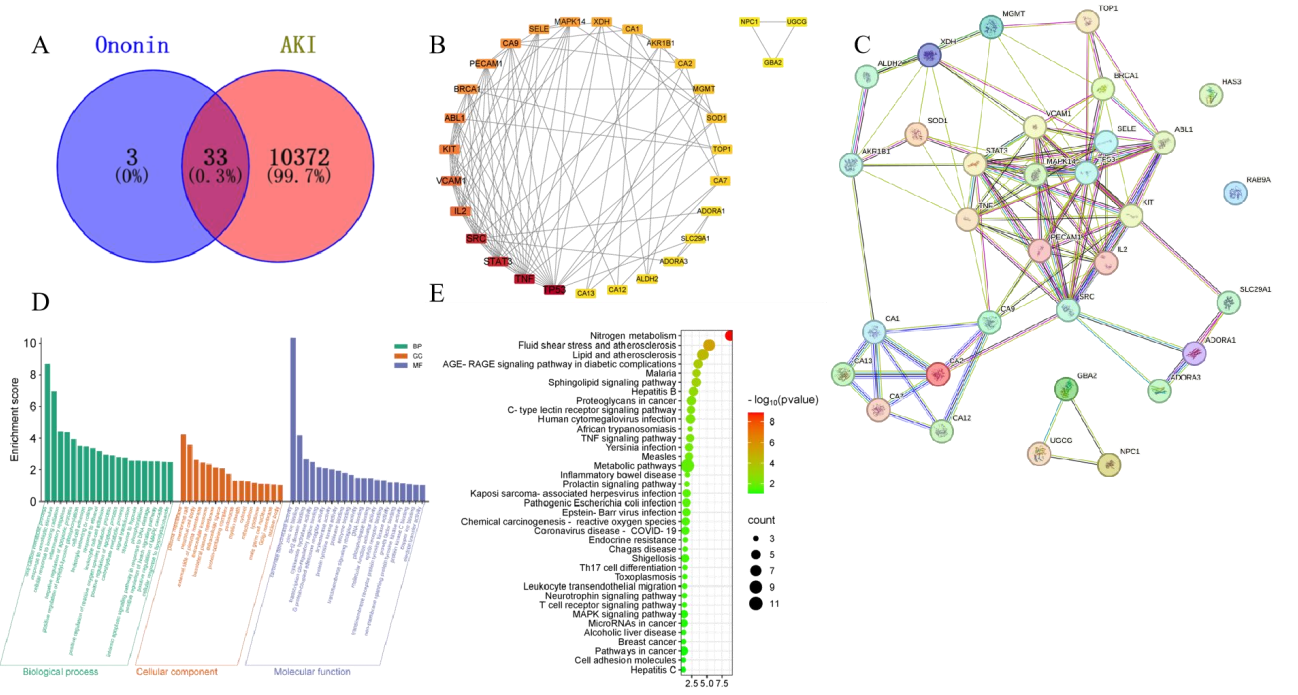

Figure 2 Network pharmacology analysis. (A) The target genes of ononin and AKI found by Veen; (B) The PPI network among the targets of ononin for the treatment of AKI; (C) The core genes of the targets of ononin for the treatment of AKI; (D) GO enrichment analysis; (E) KEGG pathway enrichment analysis. AKI, acute kidney injury; BP, biological process; CC, cellular component; MF, molecular function; PPI, protein-protein interaction.

Metascape was used to perform GO functional enrichment analysis on the common target protein genes identified above, and key functions ranked at the top were selected to create a histogram. GO enrichment analysis encompassed three categories: cellular components, biological processes, and molecular functions (Figure 2D). Biological process analysis revealed significant enrichment in processes including one-carbon metabolic process (GO: 0006730), response to xenobiotic stimulus (GO: 0009410), cellular response to ionizing radiation (GO: 0071478), and inflammatory response (GO: 0006954). Cellular component analysis identified significant associations with plasma membrane (GO: 0005886), membrane raft (GO: 0045121), and neuronal cell body (GO: 0043025). Molecular function analysis demonstrated enrichment in carbonate dehydratase activity (GO: 0004089), zinc ion binding (GO: 0008270), and SH2 domain binding (GO: 0005070).

KEGG pathway enrichment analysis was conducted using Metascape, with the most significantly enriched pathways visualized in a bubble plot (Figure 2E). KEGG pathway analysis suggested that ononin's therapeutic effects on AKI might be mediated through multiple signaling pathways and molecular targets. Bioinformatic pathway analysis revealed several critical signaling cascades potentially modulated by the intervention, most notably: the AGE-RAGE axis implicated in diabetic pathogenesis (KEGG hsa04933), tumor necrosis factor-mediated inflammatory signaling (hsa04668), T lymphocyte activation pathways (hsa04660), and the mitogen-activated protein kinase (MAPK) cascade (hsa04010).

Molecular docking

Molecular docking simulations between ononin and the screened target proteins were conducted using the HDOCK server. The docking scores, expressed as binding affinity values (kcal/mol), are summarized in Table 2.

The docking results demonstrated that mitogen-activated protein kinase 14 (MAPK14, P38 MAPK) exhibited the highest binding affinity with ononin, suggesting the strongest molecular interaction. The molecular interactions between ononin and MAPK14 were visualized using PyMOL Molecular Graphics System, illustrating key hydrogen bonds, hydrophobic interactions, and binding pocket residues (Figure 3).

Among these pathways, the MAPK signaling pathway, known for its critical role in regulating inflammatory responses, was identified as a key player in AKI progression. This finding aligns with the identification of MAPK14 (P38 MAPK) as a core target in our network pharmacology analysis. Based on the integrated analysis of molecular docking results, key target predictions, and KEGG pathway enrichment, we prioritized the MAPK signaling pathway for experimental validation.

Animal experiment verification

Effect of ononin on renal index and serum biomarkers in AKI mice. Figure 4A demonstrates a statistically significant elevation in RSI in AKI-induced animals relative to control cohorts ($P < 0.05$). Pharmacological intervention with ononin produced a dose-responsive suppression of this pathological increase, with both low- and high-dose regimens showing significant amelioration ($P < 0.05$).

Biochemical analysis revealed marked elevations in serum NGAL, Scr, and BUN concentrations in AKI-induced animals relative to control cohorts ($P < 0.05$, Figure 4B–4D). Pharmacological intervention with ononin produced a dose-dependent attenuation of these renal dysfunction biomarkers, with both treatment regimens demonstrating statistically significant reductions ($P < 0.05$).

The effect of ononin on the pathological changes in mouse kidneys. The results of HE staining are shown in Figure 5A. In the Control group, renal tissue architecture appeared normal, with intact glomeruli and well-organized tubular structures. The AKI model group exhibited significant pathological alterations, including tubular epithelial cell swelling, marked tubular dilation, and extensive inflammatory cell infiltration, resulting in disrupted renal architecture. Compared to the AKI model group, ononin-pretreated mice demonstrated attenuated renal pathology, characterized by reduced tubular epithelial cell swelling and necrosis, decreased tubular luminal space, and diminished inflammatory cell infiltration. PAS

histochemical analysis (Figure 5B) demonstrated significantly intensified staining intensity in renal tissues of the AKI model group relative to controls, indicating enhanced glycoprotein deposition. Therapeutic intervention with ononin markedly attenuated this pathological PAS reactivity across all treatment groups. The results of PAS staining (Figure 5B) showed that the positive PAS reaction was enhanced in the model group compared with the control group; after the administration of the intervention, the positive PAS reaction was weakened in all groups.

Masson's trichrome staining (Figure 5C) revealed distinct collagen deposition patterns across experimental groups: Control group kidneys exhibited negligible blue-stained collagen fibers, Model group specimens demonstrated extensive interstitial collagen deposition (blue staining), and therapeutic intervention groups showed significantly attenuated fibrotic area coverage compared to AKI models.

The transmission electron microscopy (TEM) results are shown in Figure 5D. TEM analysis revealed that renal tubular epithelial cells in the AKI model group exhibited mitochondrial swelling, localized protrusions, matrix disorganization, cristae fragmentation, and vacuolization. In contrast, the mitochondria in the Control group, Ononin-L group, Ononin-H group, and DXMS group maintained normal morphology without significant ultrastructural abnormalities.

Table 2 Docking score and confidence score

Target	Docking score	Confidence score
ABL1	−199.06	0.7273
IL2	−162.61	0.5627
MAPK14	−204.15	0.7471
STAT3	−172.23	0.6094
TP53	−132.73	0.4145
KIT	−164.83	0.5736
TNF	−163.26	0.5659
BRCA1	−184.08	0.6641
CA9	−156.84	0.5341
PECAM1	−188.98	0.6856
SELE	−200.67	0.7337

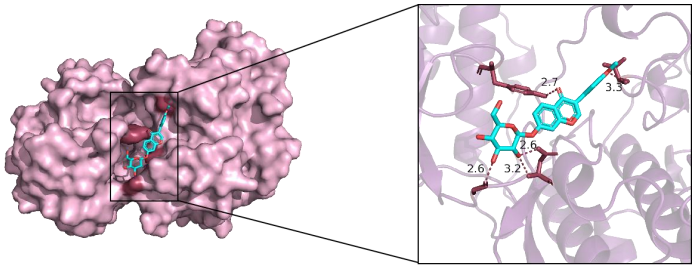

Figure 3 Molecular docking of ononin and MAPK14

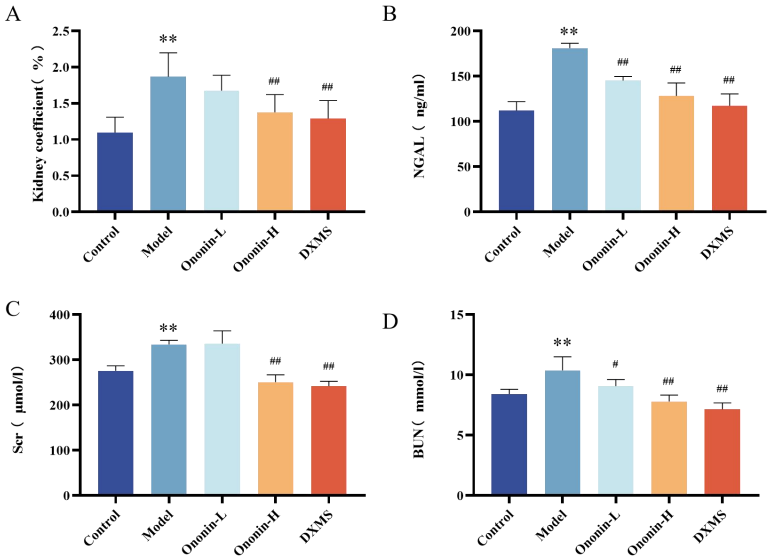

Figure 4 Ononin's effects on renal index and serum levels of NGAL, Scr, and BUN in mice with AKI (n = 3, $\bar{x} \pm s$). (A) Kidney coefficient; (B–D) Levels of serum NGAL, Scr and BUN. $^{**}P < 0.01$ vs. control group; $^{\#}P < 0.05$, $^{\#\#}P < 0.01$ vs. model group. NGAL, neutrophil gelatinase-associated lipocalin; Scr, serum creatinine; BUN, blood urea nitrogen; AKI, acute kidney injury.

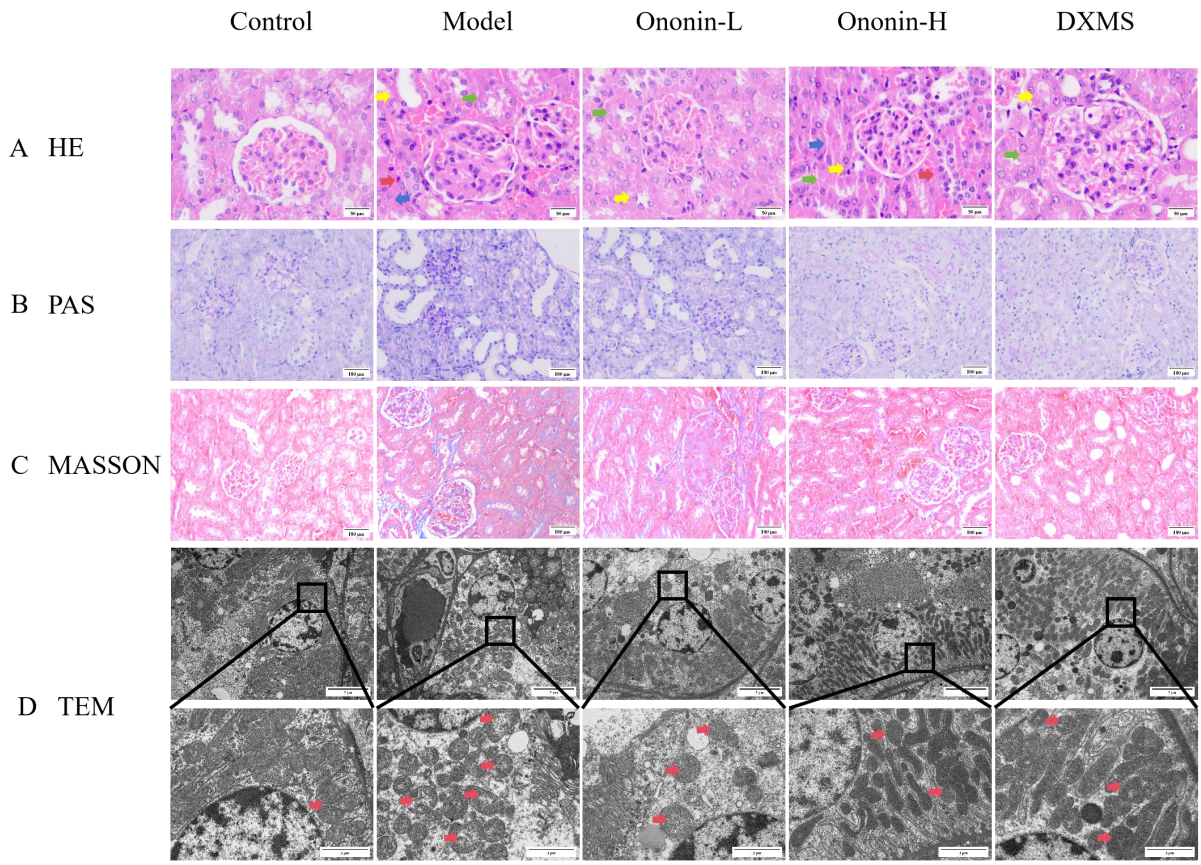

Figure 5 Effect of ononin on AKI induced renal pathological morphology alteration (n = 3). (A) Histopathological assessment of renal tissues revealed distinct morphological alterations across experimental groups (representative images shown). Key observations included: green arrows denote swollen renal tubular epithelial cells indicative of cellular edema, blue arrows highlight regions of tubular necrosis characterized by nuclear pyknosis and loss of cellular architecture, yellow arrows mark significant tubular dilation with luminal expansion, and red arrows identify focal areas of inflammatory cell infiltration (Scale bar = 50 μm); (B) PAS (Scale bar = 100 μm); (C) MASSON (Scale bar = 100 μm); (D) Transmission Electron Microscopy: Red arrows denote pathological mitochondrial alterations characterized by: organelle swelling with disrupted outer membranes, formation of clear intra-mitochondrial vacuoles, and fragmentation or complete loss of cristae structures (Scale bar = 5 μm) (Scale bar = 2 μm). DXMS, Dexamethasone; HE, hematoxylin and eosin; PAS, periodic acid-Schiff; MASSON, Masson's trichrome; TEM, transmission electron microscopy; AKI, acute kidney injury.

Immunofluorescence results of P-P38, P-ERK, NGAL and KIM-1 expression in mouse kidney tissues of each group. Immunofluorescence analysis demonstrated significantly elevated expression of renal injury biomarkers NGAL and KIM-1 in model group specimens compared to controls ($P < 0.05$), with pretreatment groups exhibiting markedly attenuated fluorescence signals.

These findings confirm both successful AKI induction and therapeutic efficacy of the intervention. Furthermore, phosphorylated P38 (P-P38) and ERK (P-ERK) expression was substantially increased in AKI models relative to baseline levels, while drug pretreatment significantly suppressed this activation ($P < 0.05$, Figure 6).

The effect of ononin on the expression of pro-inflammatory cytokines and *P38 MAPK*, *ERK*, *NGAL*, *KIM-1* mRNA in the kidneys of AKI mice. Quantitative PCR analysis revealed significant upregulation of inflammatory mediators (*IL-1β*, *IL-6*, *TNF-α*), MAPK signaling components (*P38 MAPK*, *ERK*), and renal injury markers (*NGAL*, *KIM-1*) in AKI model kidneys compared to controls ($P < 0.05$, Figure 7A–7G). Therapeutic intervention dose-dependently suppressed these transcriptional changes, with high-dose treatment demonstrating the most pronounced reductions in target gene expression ($P < 0.05$).

Effect of ononin on renal P38 MAPK, P-P38 MAPK, ERK, P-ERK, NGAK, KIM-1 protein expression in AKI mice. WB quantification (Figure 8) demonstrated significant upregulation of phosphorylated-to-total protein ratios (P-P38/P38 and P-ERK/ERK) along with elevated NGAL and KIM-1 expression in AKI model kidneys versus controls ($P < 0.05$). Therapeutic intervention significantly suppressed MAPK pathway activation, with all treatment groups showing reduced P-P38/P38 and P-ERK/ERK ratios ($P < 0.05$). Notably, both Ononin-H and DXMS treatments effectively attenuated renal injury marker expression (NGAL and KIM-1, $P < 0.05$).

Discussion

AKI is a clinical syndrome characterized by the accumulation of NGAL, BUN, and Scr, as well as disturbances in water, electrolyte, and acid-base balance [19]. Current therapeutic strategies for AKI mainly include intravenous fluid therapy, colloid therapy, improvement of renal perfusion, and RRT [20–23]. Ononin, an isoflavonoid compound isolated from the medicinal herb *Astragalus membranaceus*, exhibits potent biological activities including reactive oxygen species scavenging capacity, suppression of inflammatory mediators, and inhibition of programmed cell death pathways [24]. Studies have demonstrated that ononin improves inflammatory responses through the MAPK signaling pathways, suggesting its potential protective role in AKI [18, 25]. In this study, doxorubicin-induced AKI was successfully established via tail vein administration. Biochemical analyses revealed significant elevations in renal dysfunction markers (NGAL, BUN, Scr) in model animals compared to controls. Histopathological examination demonstrated severe tubular injury, while immunofluorescence and electron microscopy confirmed structural alterations. Molecular analyses showed: RT-qPCR detected upregulated pro-inflammatory cytokine expression, Immunoblotting revealed altered phosphorylation states of P38 MAPK/ERK signaling

proteins, and Both transcriptional and translational levels of injury biomarkers (NGAL, KIM-1) were significantly modulated. After intervention with ononin and DXMS drugs, the aforementioned results were significantly alleviated, suggesting that ononin can improve renal function in doxorubicin-induced AKI mice and reduce inflammatory responses.

Studies have demonstrated that AKI induces a rapid decline in renal function, characterized by tubular and glomerular damage, as well as

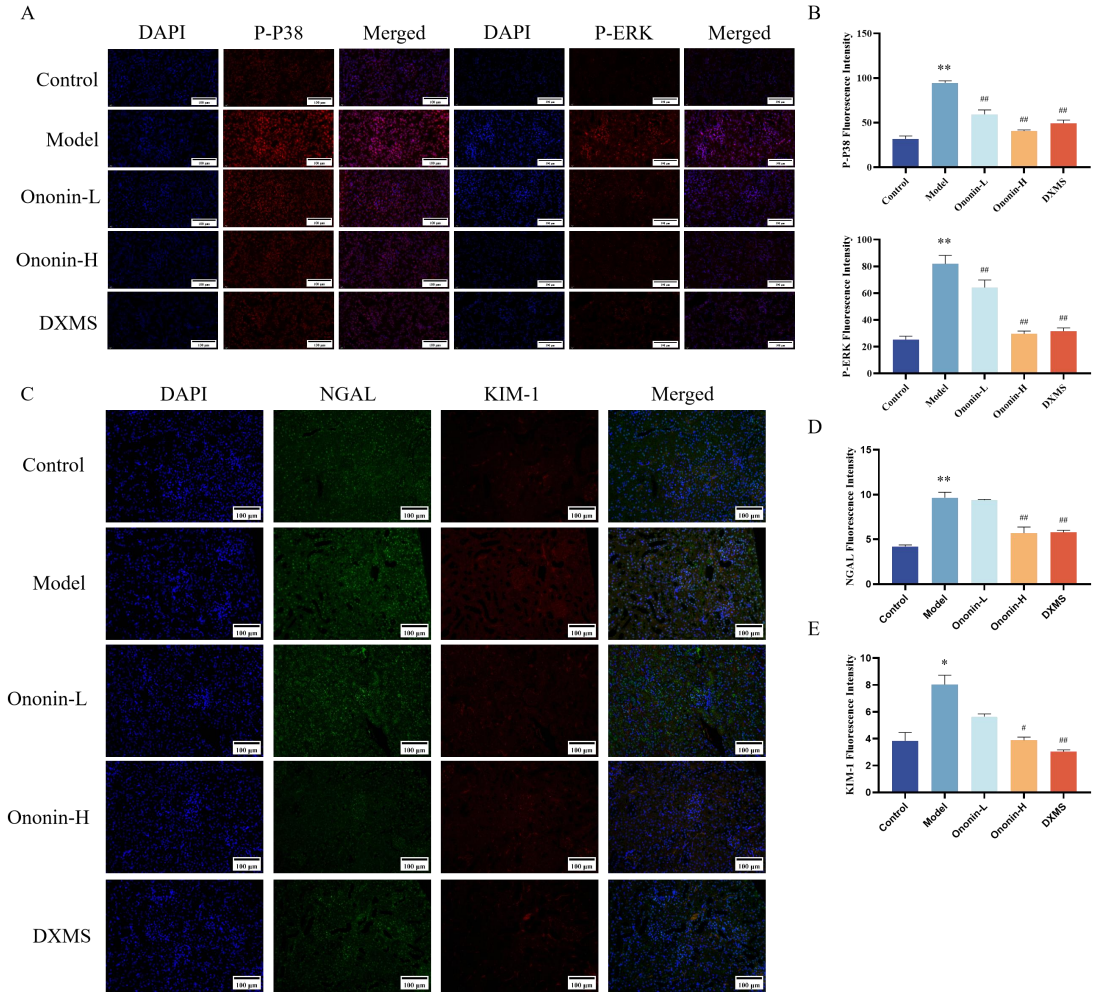

Figure 6 IF results of P-P38 , P-ERK, NGAL and KIM-1 expression in mouse kidney tissues of each group (n = 3, $\bar{x}$ ± s). (A) Representative IF staining of P-P38 (red) and DAPI (blue) in kidney tissues (Scale bar = 100 μm) and Representative IF staining of P-ERK (red) and DAPI (blue) in kidney tissues (Scale bar = 100 μm); (B) P-P38, P-ERK; (C) Representative IF staining of NGAL (green), KIM-1 (red) and DAPI (blue) in kidney tissues (Scale bar = 100 μm); (D) NGAL; (E) KIM-1. $^{*}P < 0.05$, $^{**}P < 0.01$ vs. control group; $^{\#}P < 0.05$, $^{\#\#}P < 0.01$ vs. model group. DXMS, Dexamethasone.

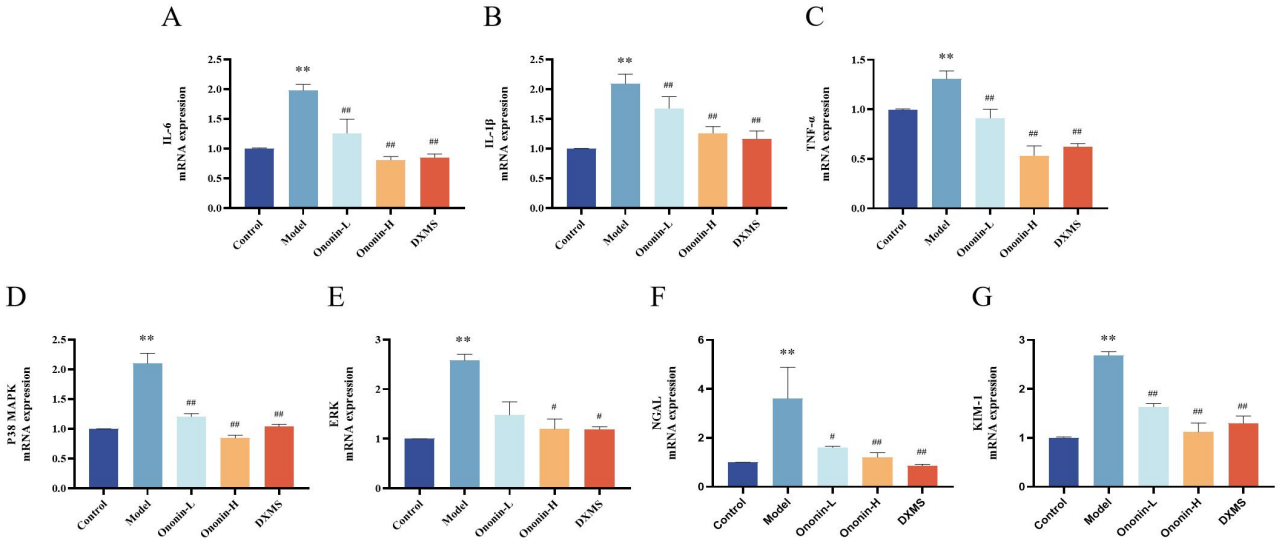

Figure 7 Ononin's effects on pro-inflammatory cytokines and *P38 MAPK*, *ERK*, *NGAL*, *KIM-1* mRNA expression in the kidneys of mice with AKI (n = 3, $\bar{x}$ ± s). $^{*}P < 0.05$, $^{**}P < 0.01$ vs. control group; $^{\#}P < 0.05$, $^{\#\#}P < 0.01$ vs. model group. DXMS, Dexamethasone.

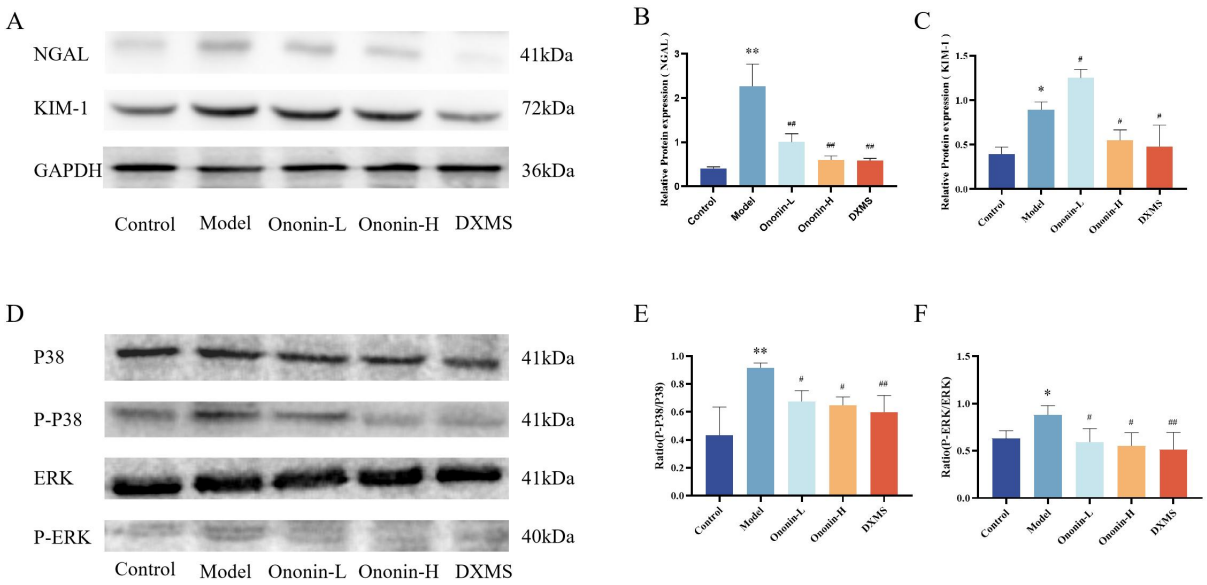

Figure 8 Effect of ononin on protein expression of P38 MAPK, P-P38 MAPK, ERK, P-ERK, NGAL and KIM-1 in AKI mice (n = 3, $\bar{x} \pm s$). $^{*}P < 0.05$, $^{**}P < 0.01$ vs. control group; $^{\#}P < 0.05$, $^{\#\#}P < 0.01$ vs. model group. DXMS, Dexamethasone.

mitrial dysfunction [14, 26]. In this experiment, it was found that the Model group mice exhibited severe tubular injury, characterized by damage to tubular epithelial cells, tubular dilation, and vacuolar degeneration. Histopathological evaluation revealed concurrent necrotic and apoptotic changes in tubular epithelium, accompanied by pronounced inflammatory cell accumulation within the renal interstitium. Ultrastructural analysis demonstrated significant mitochondrial impairment, correlating with upregulated expression of renal injury biomarkers. These findings indicate that the pathological changes in the kidneys of the AKI mouse model are consistent with the results of renal function indicators. After treatment with ononin, both tubular injury and inflammatory infiltration were significantly improved.

AKI is primarily driven by inflammatory mechanisms. Previous investigations have demonstrated that injured renal epithelial cells initiate a cascade of inflammatory signaling through the secretion of pro-inflammatory mediators, subsequently recruiting and activating immune cells [27, 28]. This process culminates in a cytokine storm marked by elevated *IL-1β*, *IL-6*, and *TNF-α* expression. Our qPCR data corroborate these findings, showing substantial upregulation of these inflammatory markers in AKI models. Notably, pharmacological intervention with ononin effectively attenuated this cytokine overexpression, confirming its robust anti-inflammatory capacity.

Prior research has established the MAPK cascade as a pivotal intracellular transduction system that orchestrates inflammatory signaling pathways [29]. P38 MAPK is a key stress-responsive kinase that significantly influences inflammatory processes in various cell types [30, 31]. Upon phosphorylation, P38 MAPK can activate a series of downstream effector molecules, leading to increased secretion of pro-inflammatory cytokines , including TNF-α and IL-6. Therefore, the activation of P38 MAPK is considered an important aspect of acute inflammatory responses [32, 33]. Additional research has demonstrated that the MAPK/ERK signaling pathway also modulates the secretion of inflammatory mediators [34]. Although ERK is traditionally associated with growth factor-induced cell proliferation and differentiation, recent studies have revealed its involvement in inflammatory responses under specific conditions [35]. This study shows that in AKI, the phosphorylation expression of the P38 MAPK/ERK pathway is elevated, while ononin can effectively inhibit these changes. These results suggest that ononin can exert anti-inflammatory and protective effects.

Conclusion

In conclusion, ononin improved renal function and reduced inflammatory damage in AKI mice, suggesting that ononin may exert its protective effects against AKI by alleviating inflammatory responses and modulating the P38 MAPK/ERK signaling pathway.

References

1. Kidney Disease: Improving Global Outcomes (KDIGO) Diabetes Work Group. KDIGO 2022 Clinical Practice Guideline for Diabetes Management in Chronic Kidney Disease. *Kidney Int.* 2022;102(5S):S1–S127. Available at: http://doi.org/10.1016/j.kint.2022.06.008
2. Kellum JA, Romagnani P, Ashuntantang G, Ronco C, Zarbock A, Anders HJ. Acute kidney injury. *Nat Rev Dis Primers.* 2021;7(1):52. Available at: http://doi.org/10.1038/s41572-021-00284-z
3. Pickkers P, Darmon M, Hoste E, et al. Acute kidney injury in the critically ill: an updated review on pathophysiology and management. *Intensive Care Med.* 2021;47(8):835–850. Available at: http://doi.org/10.1007/s00134-021-06454-7
4. Zarbock A, Koyner JL, Gomez H, et al. Sepsis-associated acute kidney injury-treatment standard. *Nephrol Dial Transplant.* 2023;39(1):26–35. Available at: http://doi.org/10.1093/ndt/gfad142
5. Chadda KR, Puthucheary Z. Persistent inflammation, immunosuppression, and catabolism syndrome (PICS): a review of definitions, potential therapies, and research priorities. *Br J Anaesth.* 2024;132(3):507–518. Available at: http://doi.org/10.1016/j.bja.2023.11.052
6. Baer PC, Koch B, Geiger H. Kidney Inflammation, Injury and Regeneration 2020. *Int J Mol Sci.* 2021;22(11):5589. Available at: http://doi.org/10.3390/ijms22115589
7. Fu Y, Xiang Y, Li H, Chen A, Dong Z. Inflammation in kidney repair: Mechanism and therapeutic potential. *Pharmacol Ther.* 2022;237:108240. Available at: http://doi.org/10.1016/j.pharmthera.2022.108240
8. Singbartl K, Formeck CL, Kellum JA. Kidney-Immune System Crosstalk in AKI. *Semin Nephrol.* 2019;39(1):96–106. Available at: http://doi.org/10.1016/j.semnephrol.2018.10.007
9. Ban KY, Nam GY, Kim D, Oh YS, Jun HS. Prevention of LPS-Induced Acute Kidney Injury in Mice by Bavachin and Its

Potential Mechanisms. *Antioxidants (Basel)*. 2022;11(11):2096. Available at: http://doi.org/10.3390/antiox11112096
10. Diao HY, Zhu W, Liu J, Yin S, Wang JH, Li CL. Salvianolic Acid A Improves Rat Kidney Injury by Regulating MAPKs and TGF-β1/Smads Signaling Pathways. *Molecules.* 2023;28(8):3630. Available at: http://doi.org/10.3390/molecules28083630
11. Wu W, Wang X, Yu X, Lan HY. Smad3 Signatures in Renal Inflammation and Fibrosis. *Int J Biol Sci.* 2022;18(7):2795–2806. Available at: http://doi.org/10.7150/ijbs.71595
12. Gałgańska H, Jarmuszkiewicz W, Gałgański Ł. Carbon dioxide and MAPK signalling: towards therapy for inflammation. *Cell Commun Signal.* 2023;21(1):280. Available at: http://doi.org/10.1186/s12964-023-01306-x
13. Livingston MJ, Zhang M, Kwon SH, et al. Autophagy activates EGR1 via MAPK/ERK to induce FGF2 in renal tubular cells for fibroblast activation and fibrosis during maladaptive kidney repair. *Autophagy.* 2023;20(5):1032–1053. Available at: http://doi.org/10.1080/15548627.2023.2281156
14. Ishimoto Y, Inagi R. Mitochondria: a therapeutic target in acute kidney injury. *Nephrol Dial Transplant.* 2016;31(7):1062–1069. Available at: http://doi.org/10.1093/ndt/gfv317
15. Yu T, Lu X, Liang Y, Yang L, Yin Y, Chen H. Ononin alleviates DSS-induced colitis through inhibiting NLRP3 inflammasome via triggering mitophagy. *Immun Inflamm Dis.* 2023;11(2):e776. Available at: http://doi.org/10.1002/iid3.776
16. Chen X, Zhang M, Ahmed M, Surapaneni KM, Veeraraghavan VP, Arulselvan P. Neuroprotective effects of ononin against the aluminium chloride-induced Alzheimer's disease in rats. *Saudi J Biol Sci.* 2021;28(8):4232–4239. Available at: http://doi.org/10.1016/j.sjbs.2021.06.031
17. Pan R, Zhuang Q, Wang J. Ononin alleviates H_2O_2-induced cardiomyocyte apoptosis and improves cardiac function by activating the AMPK/mTOR/autophagy pathway. *Exp Ther Med.* 2021;22(5):1307. Available at: http://doi.org/10.3892/etm.2021.10742
18. Meng Y, Ji J, Xiao X, et al. Ononin induces cell apoptosis and reduces inflammation in rheumatoid arthritis fibroblast-like synoviocytes by alleviating MAPK and NF-κB signaling pathways. *Acta Biochim Pol.* 2021;68(2):239–245. Available at: http://doi.org/10.18388/abp.2020_5528
19. Zhao Y, Feng X, Li B, et al. Dexmedetomidine Protects Against Lipopolysaccharide-Induced Acute Kidney Injury by Enhancing Autophagy Through Inhibition of the PI3K/AKT/mTOR Pathway. *Front Pharmacol.* 2020;11:128. Available at: http://doi.org/10.3389/fphar.2020.00128
20. Moore PK, Hsu RK, Liu KD. Management of Acute Kidney Injury: Core Curriculum 2018. *Am J Kidney Dis.* 2018;72(1):136–148. Available at: http://doi.org/10.1053/j.ajkd.2017.11.021
21. Myles PS, Bellomo R, Corcoran T, et al. Restrictive versus Liberal Fluid Therapy for Major Abdominal Surgery. *N Engl J Med.* 2018;378(24):2263–2274. Available at: http://doi.org/10.1056/NEJMoa1801601
22. Self WH, Semler MW, Bellomo R, et al. Liberal Versus Restrictive Intravenous Fluid Therapy for Early Septic Shock: Rationale for a Randomized Trial. *Ann Emerg Med.* 2018;72(4):457–466. Available at: http://doi.org/10.1016/j.annemergmed.2018.03.039
23. Silversides JA, Major E, Ferguson AJ, et al. Conservative fluid management or deresuscitation for patients with sepsis or acute respiratory distress syndrome following the resuscitation phase of critical illness: a systematic review and meta-analysis. *Intensive Care Med.* 2016;43(2):155–170. Available at: http://doi.org/10.1007/s00134-016-4573-3
24. Mladenova SG, Savova MS, Marchev AS, et al. Anti-adipogenic activity of maackiain and ononin is mediated via inhibition of PPARγ in human adipocytes. *Biomed Pharmacother.* 2022;149:112908. Available at: http://doi.org/10.1016/j.biopha.2022.112908
25. Xu F, Zhao LJ, Liao T, et al. Ononin ameliorates inflammation and cartilage degradation in rat chondrocytes with IL-1β-induced osteoarthritis by downregulating the MAPK and NF-κB pathways. *BMC Complement Med Ther.* 2022;22(1):25. Available at: http://doi.org/10.1186/s12906-022-03504-5
26. Wang Z, Wu J, Hu Z, et al. Dexmedetomidine Alleviates Lipopolysaccharide-Induced Acute Kidney Injury by Inhibiting p75NTR-Mediated Oxidative Stress and Apoptosis. *Oxid Med Cell Longev.* 2020;2020:5454210. Available at: http://doi.org/10.1155/2020/5454210
27. Linfert D, Chowdhry T, Rabb H. Lymphocytes and ischemia-reperfusion injury. *Transplant Rev.* 2009;23(1):1–10. Available at: http://doi.org/10.1016/j.trre.2008.08.003
28. Ning EJ, Sun CW, Wang XF, et al. Artemisia argyi polysaccharide alleviates intestinal inflammation and intestinal flora dysbiosis in lipopolysaccharide-treated mice. *Food Med Homol.* 2024;1(1):9420008. Available at: http://doi.org/10.26599/FMH.2024.9420008
29. Min YP, Sang EH, Hun HK, et al. Scutellarein Inhibits LPS-Induced Inflammation through NF-κB/MAPKs Signaling Pathway in RAW264.7 Cells. *Molecules.* 2022;27(12):3782. Available at: http://doi.org/10.3390/molecules27123782
30. Plastira I, Bernhart E, Joshi L, et al. MAPK signaling determines lysophosphatidic acid (LPA)-induced inflammation in microglia. *J Neuroinflammation.* 2020;17(1):127. Available at: http://doi.org/10.1186/s12974-020-01809-1
31. Singh SP, Dosch AR, Mehra S, et al. Tumor Cell-Intrinsic P38 MAPK Signaling Promotes IL1α-Mediated Stromal Inflammation and Therapeutic Resistance in Pancreatic Cancer. *Cancer Res.* 2024;84(8):1320–1332. Available at: http://doi.org/10.1158/0008-5472.CAN-23-1200
32. Falcicchia C, Tozzi F, Arancio O, Watterson DM, Origlia N. Involvement of P38 MAPK in Synaptic Function and Dysfunction. *Int J Mol Sci.* 2020;21(16):5624. Available at: http://doi.org/10.3390/ijms21165624
33. Mai L, Zhu X, Huang F, He H, Fan W. p38 mitogen-activated protein kinase and pain. *Life Sci.* 2020;256:117885. Available at: http://doi.org/10.1016/j.lfs.2020.117885
34. Wang Y, Han D, Huang Y, et al. Oral administration of punicalagin attenuates imiquimod-induced psoriasis by reducing ROS generation and inflammation via MAPK/ERK and NF-κB signaling pathways. *Phytother Res.* 2023;38(2):713–726. Available at: http://doi.org/10.1002/ptr.8071
35. Dong N, Li X, Xue C, et al. Astragalus polysaccharides alleviates LPS-induced inflammation via the NF-κB/MAPK signaling pathway. *J Cell Physiol.* 2020;235(7–8):5525–5540. Available at: http://doi.org/10.1002/jcp.29452